# Nonlinear immunofluorescent assay for androgenic hormones based on resonant structures

**Anisha Thayil K. N.[1], Alejandro Muriano,[2] J.-Pablo Salvador[2], Roger Galve[2], Maria Pilar Marco[2], Dobryna Zalvidea[1], Pablo Loza-Alvarez[1], Tsvi Katchalski[3], Eran Grinvald[3], Asher A. Friesem[3] and Silvia Soria[4*]**

*[1]ICFO-Institut de Ciencies Fotoniques, Ada. Canal Olimpic s/n, 08600 Castelldefels, Barcelona, Spain*
*[2]Applied Molecular Receptors Group, CSIC, CIBER of Bioengineering, Biomaterials and Nanomedicine, 08034-Barcelona, Spain*
*[3] Department of Physics of Complex Systems, Weizmann Institute of Science, 76100 Rehovot, Israel*
*[4]Centro Studi e Ricerche "Enrico Fermi"00184 Rome and "N. Carrara" Institute of Applied Physics -CNR ,50019 Sesto Fiorentino (FI), Italy*
*[*]Corresponding author: s.soria@ifac.cnr.it*

**Abstract**: We report for the first time the use of two photon fluorescence as detection method of affinity binding reactions. We use a resonant grating waveguide structure as platform enhancement for detecting the interaction between fluorescent labeled Boldenone, a non-natural androgenic hormone, and a specific anti-anabolic antibody. We were able to detect a surface coverage of approximately 0.7 ng/mm$^2$.



**OCIS codes:** (130.6010) Sensors; (230.5750) Resonators; (170.4520) Optical Confinement and manipulation; (190.1900) Diagnostics Applications of Non linear Optics.

## References and links

1. J. Tschmelak, M. Kumpf, N. Kappel, and G. Proll, "Total internal reflectance fluorescence (TIRF) biosensor for environmental monitoring of testosterone with commercially available immunochemistry: Antibody characterization, assay development and real sample measurements," Talanta. **69**, 343-350 (2006)
2. M. Kreuzer, R. Quidant, J.-P. Salvador, M.-P. Marco, and G. Badenes, "Colloidal-based localized surface plasmon resonance (LSPR) biosensor for the quantitative determination of stanozolol," Anal. Bioanal. Chem. **391**, 1813-1820 (2008).
3. T. E. Plowman, W. M. Reichert, C. R. Peters, H. K. Wang, D. A. Christensen and J. N. Herron, "Femtomolar sensitivity using a channel etched thin film waveguide as fluoroimmunosensor," Biosens. Bioelectron. **11,** 149-160 (1996).
4. S. Soria, T. Katchalski, E. Teitelbaum, A. A. Friesem, and G. Marowsky, "Enhanced two photon fluorescence excitation by resonant grating waveguide structures," Opt. Lett. **29**, 1989-1991 (2004).
5. A. Selle, C. Kappel, M. A. Bader, G. Marowsky, K. Winkler and U. Alexiev, "Picosecond-pulse-induced TPF enhancement in biological material by application of grating waveguide structures," Opt. Lett. **30,** 1683-1685 (2005).
6. S. Soria, A. Thayil K. N., G. Badenes, M. A. Bader, A. Selle and G. Marowsky, "Resonant double grating waveguide structures as enhancement platforms for two photon fluorescence excitation," Appl. Phys. Lett. 87, 081109 (2005).
7. G. L. Duveneck, M. A. Bopp, M. Ehrat, M. Haiml, U. Keller, M. A. Bader, G. Marowsky, and S. Soria, "Evanescent-fiel-induced two-photon fluorescence: excitation of macroscopic areas of planar waveguides," Appl. Phys. B, 73, 869-871 (2001).
8. M. T. Myaing, J. Y. Ye, T. B. Norris, T. Thomas, J. R. Baker Jr, W. J. Wadsworth, G. Bouwmans, J. C. Knight and P. St. J. Russell, "Enhanced two photon biosensing with double-clad photonic crystal fibers," Opt. Lett. **28**, 1224-1226 (2003).
9. W. Budach, D. Neuschaefer, C. Wanke, and S. Chibout, "Generation of Transducers for Fluorescence based microarrays with enhanced sensitivity and their application for gene expression profiling," Anal. Chem. **45**, 2571-2577 (2003).
10. D. Neuschaefer, W. Budach, C. Wanke, and S. Chibout, "Evanescent resonator chips: a universal platform with superior sensitivity for fluorescence-based microarrays," Biosens. Bioelectron. **18**, 489-497 (2003).
11. R. Wood, "On a remarkable case of uneven distribution of light in a diffraction grating spectrum," Phil. Mag. **4**, 396-408 (1902).
12. h124RE BioChip.pdf from www.optics.unaxis.com

#98971 - $15.00 USD Received 17 Jul 2008; revised 8 Aug 2008; accepted 8 Aug 2008; published 13 Aug 2008

13. D. Brovelli, G. Hahner, L. Ruiz, R. Hofer, G. Kraus, A. Waldner, J. Schlosser, P. Oroszlan, M. Ehrat, and N. D. Ehrat, "Highly Oriented, Self-Assembled Alkanephosphate Monolayers on Tantalum(V) Oxide Surfaces," Langmuir. **15**, 4324-4327 (1999)
14. K. O. Katrin, K. O. Schmitt, G. Sulz, and C. Hoffmann, "Evanescent field Sensors Based on Tantalum Pentoxide Waveguides - A review," Sensors. **8**, 711-738 (2008).
15. Specific antibody (Ab143) and non-specific antibody (Abpre) were previously produced in the AMR research group by Dr. J.-P. Salvador.
16. A. Muriano, A. Thayil K. N., P. Salvador, R. Galve, S. Soria, P. Loza-Alvarez and M. P. Marco, Anal. Chem., in preparation
17. U. Fano, "Effects of configuration interaction on intensities and phase shifts," Phys. Rev. **124**, 1866-1878 (1961).
18. U. Fano, " The theory of anomalous diffraction gratings and quasi stationary waves on metallic surfaces (Sommerfeld's waves)," J. Opt. Soc. Am. **31**, 213-222 (1941)
19. S. Glasberg, A. Sharon, D. Rosenblatt, and A. A. Friesem, "Spectral shifts and line-shapes asymmetries in resonant response of grating waveguide structures," Opt. Commun. **145**, 291-299 (1998).
20. S. H. Fan, W. Suh, and J. D. Joannopoulos, "Temporal coupled-mode theory for the Fano resonance in optical resonators," J. Opt. Soc. Am. A **20**,569-572 (2003).

## 1. Introduction

Boldenone and methylbodenone are anabolic steroids often illegally used as growth promoters in animals for human consumption. Due to their potential health risk in consumers, the use of natural and synthetic hormones is banned in the European Union (Directive 88/146/EEC). Moreover the use of androgenic steroids with anabolic effect to improve athletic performance has been banned by the International Olympic Committee (IOC) and other international sports associations (IAAF) since 1974. Therefore, the development of sensitive and robust methods for detecting such hormones is very important both in doping and food safety controls.

During the last years a number of optical sensors have been developed for the detection of bioaffinity reactions, either based on luminescent methods such as fluorescence [1] or on label-free methods such as changes in index of refraction [2]. Luminescent methods are independent of molecules dimensions and can be done in very small volumes. Among these, one photon fluorescence (OPF) techniques have shown impressive detection limits [3]. However, sensors using OPF suffer from the requirement of a large sensing length, noisy signal due to small stokes shift and autofluorescence of many biomolecules. More recently, two photon fluorescence (TPF) techniques exploiting the advantages of nonlinearities have been performed [4-7]. Unfortunately, TPF excitation usually requires high photon density available only at the tight focus of ultrashort laser pulses. Recently it was demonstrated that using enhancement platforms such as optical resonators TPF signals were 300-fold enhanced without the need of focusing the laser pulses [6]. To amplify TPF signal, several enhancement platforms have been developed. Among them we can find planar waveguides [7], photonic crystal fibers [8] grating waveguide structures (GWS) [4, 5] and double grating waveguide structures (DGWS) [6]. The application of DGWS to biosensing has been proposed and demonstrated with OPF as an analytical tool [9, 10].

Here we present the first experimental demonstration of a DGWS as nonlinear immunosensor. We exploit commercially available DGWS that are comprised of a multilayered structure: two gratings and a thin waveguide layer. A DGWS show an abnormal reflection [11], which stems from the destructive interference between the diffracted and the directly transmitted wave when a guided mode is excited in the waveguide. At resonance the normally transparent structure becomes highly reflective. Since the DGWS extends over a large area with a homogeneous resonance behavior [10], it is possible to attach at the surface a microtiter well plate. Thus, we could fill different wells with different antibody–antigen concentrations, leave some blank wells to serve as controls, and measure the resonance behavior of all concentrations with only one DGWS.

Like most of the platforms used for biosensing, the surfaces of the DGWS require chemical modification in order to provide a biological interface. The surface functionalization provides the covalent immobilization of the antibody/antigen and prevents non-specific binding recognition. In the following we describe in section 2 materials and methods, which include the device, the surface functionalization and the experimental set-up. In section 3 the

#98971 - $15.00 USD Received 17 Jul 2008; revised 8 Aug 2008; accepted 8 Aug 2008; published 13 Aug 2008

experimental results and discussion. Finally, in section 4 we present some concluding remarks.

## 2. Materials and methods

### *2.1 The DGWS*

The DGWS sensor transducer used in this work, which is available commercially (Unaxis Balzers, Liechtenstein), is presented schematically in Fig. 1. It consists of a glass substrate (Schott AF45, refractive index, $n$ =1.52 at 800nm) with a uniformly etched sub-micron diffraction grating. The grating has a period of 360 nm and a depth of 40nm [12]. Afterwards a thin film layer of 150nm $Ta_2O_5$ ($n$=2.09 at 800nm) is deposited in which a second identical grating is formed. In our DGWS, atomic force microscopy (AFM) measurements of the surface revealed a uniform grating with a slightly different period of 388nm and a groove depth of 38nm (inset Fig. 1). Under resonance conditions, i.e. for a certain combination of wavelength, polarization and angle of incidence, DGWS show vanishing transmission, leading to almost total reflection of the incident light. This effect is due to the destructive interference between the zero order transmitted beam and the first diffracted orders in the grating and waveguide layers.

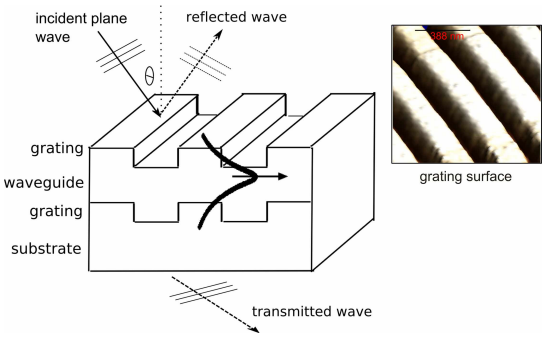


Fig. 1. A schematic diagram of the DGWS with the inset showing AFM image of a 1x1 μm section of DGWS surface. The period of the structure is 388nm and the groove depth is 38nm.The size of the transducer is 22x75 mm and 1.1mm thickness.

### *2.2 Surface functionalization.*

We first cleaned the DGWS sample with a 7:3 solution of $H_2SO_4$:$H_2O_2$ for 10 min at room temperature, gently washed with $H_2O$ milliQ and anhydrous butanol, and dried under $N_2$-stream. Then, they were immersed in a 6-phosphonohexanoic acid solution (500μM, butanol anh.) for 2h, rinsed thoroughly in butanol and dried under $N_2$-stream [13,14]. The DGWS were then immersed in a carboxilic activation solution 1-(3-(dimethylamino)-propyl)-3-ethylcarbodiimide hydrochloride (EDC) 50mM, N-hidroxisuccinimide (NHS) 25mM, in 25mM 2-(N-morpholino) of ethanesulfonic acid (MES) buffer pH 6 for 1h, washed gently with HCl 2mM and dried under $N_2$-stream. They were then fitted in an array support (ArrayIt®,TeleChem International, Inc. CA, USA). Then, four different dilutions of specific and non-specific antibodies [15] were coated overnight at room temperature under agitation conditions (from 10 to 1.25 μg/ml in phosphate buffer, pH 7.5, 150 μl/well), and washed 3 times with PBST 10mM (phosphate buffer saline, 0.05% Tween 20, pH 7.5, 200 μl/well).

The antibody affinity was evaluated by using a Rhodamine B labeled Boldenone derivative. Three different dilutions of the fluorescent conjugate (from 5 to 1.25 μg/ml in PBST containing 20% ethanol, 150 μl/well) were tested for 1h at room temperature protected from light under agitation conditions. Then, the samples were washed 3 times with PBST (200μl/well) and $H_2O$ milliQ, and dried under $N_2$-stream, as illustrated in Fig. 2. All the reagents were provided by Sigma-Aldrich. Boldenone was provided by Sequoia Research

#98971 - $15.00 USD Received 17 Jul 2008; revised 8 Aug 2008; accepted 8 Aug 2008; published 13 Aug 2008

Products Ltd, U.K. Details on the hapten synthesis and the chemical characterization are published elsewhere [16].

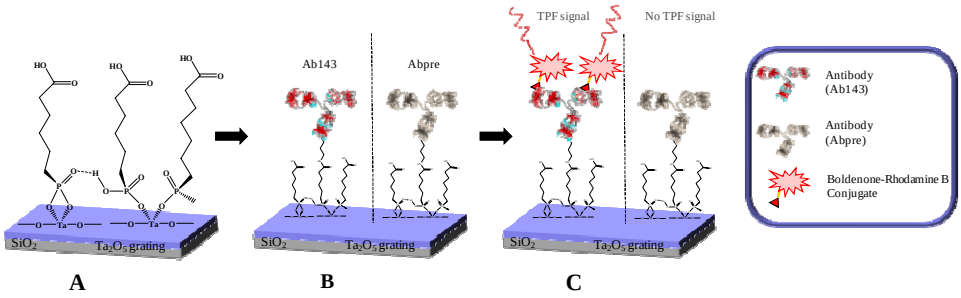


Fig. 2. Surface functionalization. (A) Schematic diagram of surface functionalization; (B) covalent protein (Ab143 specific antibody, Abpre non specific antibody) immobilization; and (C) bioaffinity assay.

*2.3 Experimental set up*

A schematic diagram of the experimental arrangement used for TPF measurements [4, 6] is shown in Fig. 3. It consisted of a non-amplified mode-locked Ti: Sapphire (Coherent, Mira 900f) producing 150 fs pulses of 8 nm spectral bandwidth at a repetition rate of 76MHz with an average power up to 1.2W. It was tuneable over a wavelength range of 690-980nm. The polarization of the laser was controlled by the combination of a polarizer and a λ/2 waveplate.

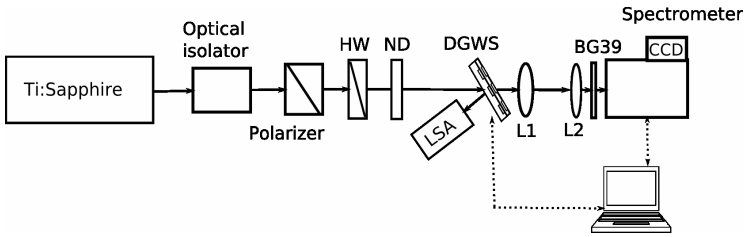


Fig. 3. A schematic diagram of the experimental arrangement. HW: half wavelength plate, ND: Neutral density filter, LSA: laser spectrum analyser, L1 and L2 collecting lenses.

The DGWS was mounted on a positioning stage (Physik Instrumente), which allowed transverse and vertical translation and a rotational stage in order to ensure accurate angle of incidence. A laser spectrum analyser was used to measure the reflected pulse spectrum from the DGWS during resonance. For the TPF measurements a collimated laser beam of 1.5 mm diameter was incident on the DGWS. The laser average power was attenuated to 450mW. The TPF signal was collected using a spherical lens ($f$=50mm, NA=0.65) and a second lens ($f$= 125mm) was used to focus the signal onto the detection system that consisted of a spectrometer (Jobin Yvon, Triax 180) combined with a double cooled back-thinned CCD linear array (Hamamatsu, HC230-1007). The excitation light was filtered in front of the entrance slit by a BG39 Schott filter.

## 3. Experimental results and discussion

The resonant behaviour of the DGWS was characterized by its transmission spectra. The measured and calculated results are presented in Fig. 4. Figure 4(a) shows that for TE polarization and at 36˚ incident angle, resonance of a bare DGWS could be observed at 812.7nm central wavelength with a resonance bandwidth of 3.3nm. For the same wavelength and incident angle, changing the polarization to TM resulted in full transmittance of the incident pulse (non- resonant condition). Figure 4(b) shows that for TM polarization, at the

#98971 - $15.00 USD Received 17 Jul 2008; revised 8 Aug 2008; accepted 8 Aug 2008; published 13 Aug 2008

same 812.7nm wavelength, the resonance occurred at a higher incident angle of 45˚, with a full width half maximum (FWHM) of 1.3nm. At 45˚ incident angle, TE polarization was non-resonant. The pulse in non-resonant condition was used for normalizing the experimental data.

We used TE polarization at an angle of incidence of 36° for the resonant enhancement of TPF excitation. In this case, due to the broader resonance bandwidth, coupling efficiency is higher than in the case TM polarisation and a larger portion of the incident pulse is coupled into the waveguide. Thus, the evanescent field intensity increases, the pulse duration of coupled light is still within the femtosecond range, and its relatively high peak intensity is maintained [6]. Consequently, the TPF signal is enhanced.

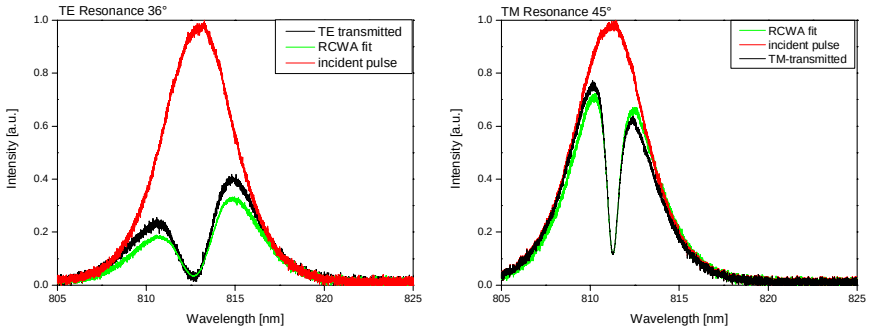


Fig. 4. Transmission spectra of a bare DGWS. (a) At 36˚ incident angle and TE polarization resonance occurs at 812.7nm wavelength with a FWHM bandwidth of 3.3nm; changing the polarization to TM results in full transmittance of the incident pulse. (b) Resonance for TM polarization at this wavelength occurs at 45˚incident angle with 1.3nm FWHM. TE polarization at this angle is a non-resonant condition.

In addition to the experimental measurements, we performed numerical calculations based on the rigorous coupled wave analysis (RCWA). The data used for the calculations is taken from subsection 2.1. As evident from Fig. 4(a) and Fig. 4(b), the calculated results (curves in green) are in very good agreement. We have added some losses, as an imaginary part of the refraction index (k=0.0022), in our RCWA numeric simulations for a more realistic situation.

We tested DGWS for monitoring affinity-binding immunoreactions between the antibody immobilized on the grating surface and the conjugated hb-Boldenone. A direct format was used with 0.3125µg/ml of antibody covalently bound to the grating surface (surface coverage of 0.7 ng/mm$^2$) to which 5µg/ml of Rhodamine B labelled hb-Boldenone was added. Figure 5 shows the spectral response of a DGWS after immunoreactions. For TE polarization and at 36˚ incident angle, resonance occurred at 814.8nm central wavelength. The shift in the resonance wavelength compared to a bare DGWS was due to the change in the refractive index when attaching biomolecules on the surface. The RCWA calculations show that the addition of a 15nm thick layer (refractive index, $n$ =1.5) will lead to a shift of approximately 2nm in the resonant wavelength.

#98971 - $15.00 USD Received 17 Jul 2008; revised 8 Aug 2008; accepted 8 Aug 2008; published 13 Aug 2008

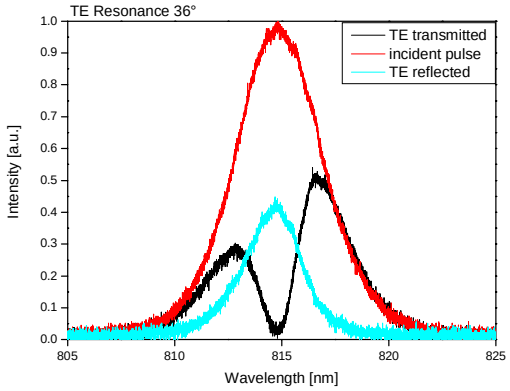


Fig. 5. Transmission and reflection spectra of a DGWS with 0.3125μg/ml of antibody and 5μg/ml of hb-Boldenone labelled with Rhodamine B. For TE polarization resonance occurs at 36˚ where TM polarization is a non-resonant condition.

As evident from Figs. 4 and 5, the resonances are asymmetric and resemble the Fano resonances that involve interference between a continuum and a discrete level [17]. Fano resonances appear in several structures like metallic and dielectric gratings [18, 19], and photonic crystal slabs [20]. In our case, the Fano-like resonances can be attributed to the interference in the waveguide between one mode and another that is reflected by the second grating and delayed by a phase shift, producing a non-quadratic term in the transmittance and reflectance [19,20]. The non-quadratic term vanishes when one of the gratings is completely transparent or fully reflecting.

Keeping the polarization and incident angle at resonance conditions, we collected TPF signal from Rhodamine B labelled hb-Boldenone bound to the antibody by tuning the laser wavelength around the resonance wavelength (i.e., 814.8nm). The results are presented in Fig. 6. Figure 6(a) shows the spectrally resolved TPF signal for different excitation wavelengths. As expected, near and at resonance a TPF signal from the DGWS was readily observed and far away from resonance no TPF signal could be observed. For non-resonant excitation (TM polarization) the signal was at the background level. Figure 6(b) shows the integrated TPF intensity as a function of the excitation wavelength. As evident, maximum TPF signal (300-fold field enhancement) was obtained when the excitation wavelength was the same as the resonance wavelength. This was quantified by comparing the TPF signal on and off resonance (off resonance the TPF signal is at the same level of background noise) with a reference sample (see for details [6]). Other nonlinear effects like surface second harmonic generation could be excluded since no signal could be detected in the spectral region between 350 and 500nm.

#98971 - $15.00 USD Received 17 Jul 2008; revised 8 Aug 2008; accepted 8 Aug 2008; published 13 Aug 2008

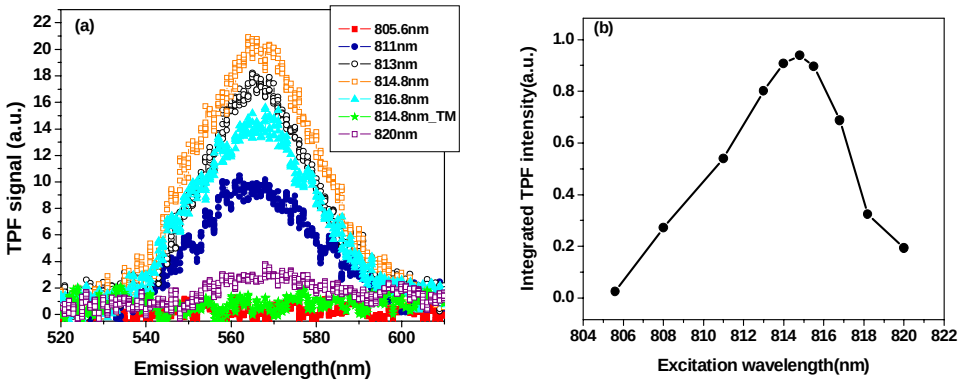


Fig. 6. TPF enhancement near resonance. (a) TPF emission spectra obtained from a DGWS with 0.3125μg/ml of antibody and 5μg/ml of Rhodamine B labelled hb-Boldenone on the grating surface for different excitation wavelengths. (b) The corresponding normalized TPF excitation spectrum.

We evaluated the potential of this immunosensor device by measuring the TPF signal variation of the immunoaffinity binding reaction. Several concentrations of covalently linked antibody and different concentrations of our fluorescent compound were tested. At 36° incident angle and TE polarization, the resonance wavelengths corresponding to different concentrations were within the range 814 ± 1nm. For TPF measurements, the excitation wavelength was tuned to the respective resonance wavelength of each concentration. Figure 7 shows the integrated TPF intensity as a function of the concentration of the specific antibody Ab143 and the non-specific one, Abpre, against Boldenone-Rhodamine B conjugate. The results show a dependency on the fluorescent-labelled-boldenone concentration and a high affinity of the specific antibody compared with the non-specific one, clearly demonstrated for lower fluorescent derivative concentrations.

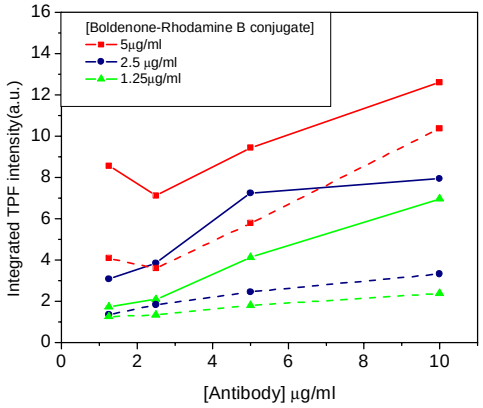


Fig. 7. Variation of the total TPF intensity for different antibody and Boldenone-Rhodamine B conjugate concentrations (squares: 5μg/ml, circles: 2.5μg/ml, triangles: 1.25 μg/ml,) Continuous line corresponds to specific Ab143, and discontinuous line corresponds to non-specific antibody Abpre. Same colour corresponds to the same concentration of fluorescent conjugate.

## 4. Conclusions

Our experiments demonstrate that DGWS are robust enhancement sensing platforms. The DGWS show resonances that are responsible for the high TPF enhancement. By taking advantage of the broad FWHM of the Fano resonances, we were able to measure for the first

#98971 - $15.00 USD Received 17 Jul 2008; revised 8 Aug 2008; accepted 8 Aug 2008; published 13 Aug 2008

time, according to our knowledge, an affinity reaction between a non-natural labelled anabolic steroid and its specific antibody by means of nonlinear detection. Significantly different TPF signals were obtained from specific and non-specific antibody against the fluorescent conjugate. We believe that non-linear detection techniques like TPF combined with resonant structures can become an important tool in doping and food safety controls. Our results suggest that in the near future it should be possible to try to develop a novel competitive immunoassay for the detection of anabolic steroids and other xenobiotic compounds.

**Acknowledgments**

A. Thayil and A. Muriano contributed equally to this work. S. Soria, A. Thayil, J.-P. Salvador and R. Galve acknowledge funding from Fundación Ramón Areces through the HINAN project, S. Soria and A. Thayil also acknowledge MEC through the PANOPTES project, S. Soria acknowledges funding and support from Centro Studi e Ricerche "E. Fermi". D. Zalvidea acknowledges MEC through Ramon y Cajal program.

#98971 - $15.00 USD Received 17 Jul 2008; revised 8 Aug 2008; accepted 8 Aug 2008; published 13 Aug 2008